ASTRONOMICAL DATA ANALYSIS SOFTWARE AND SYSTEMS XIV
ASP Conference Series, Vol. 347, 2005
P. L. Shopbell, M. C. Britton, and R. Ebert, eds.

Image Segmentation and Denoising Based on Shrira-Pesenson Equation

M. Pesenson, M. Moshir, D. Makovoz, D. Frayer, and D. Henderson

Spitzer Science Center (SSC), California Institute of Technology

Abstract. We propose a nonlinear partial differential equation to control the trade-off between smoothing and segmentation of images. Its solutions approximate discontinuities, thus leading to detection of sharp boundaries in images. The performance of the approach is evaluated by applying it to images obtained by the Multiband Imaging Photometer for *Spitzer* (MIPS), 70μm imaging band.

1. Introduction

The principal goals of image enhancement are noise removal, or smoothing, and recognition of objects of interest, which is also called image segmentation. These operations are not independent and their connection is the source of major difficulties encountered in the field of image processing. The trade-off is inevitable, and a balance between these two desirable but incompatible objectives depends on a specific application. The traditional approach to the noise removal problem ignores this connection by simply convolving an image with a Gaussian. Though such approach effectively removes noise, at the same time, it drastically smears point sources and blurs boundaries and edges. The first breakthrough in tackling this problem was achieved by Witkin (1983), who recognized that convolving an image with a Gaussian, is equivalent to solving a Cauchy problem for the linear partial differential equation (PDE) of diffusion with the noisy image as initial condition, thus explaining the blurring of boundaries, as one would expect from diffusion. This insight has led to the construction of multi-scale representations of image data.

2. A Multi-scale Representation of Images by Using PDEs

The multi-scale representations of image data are obtained by embedding the given image into a one-parameter family of derived images. This family should be parameterized by a scale parameter and be generated in such a way that fine-scale structures are successively suppressed when the scale parameter is increased. Such construction allows to obtain a separation of the image structures in the original image, such that fine scale image structures only exist at the finest scales in the multi-scale representation thus simplifying the task of object detection. This objective can be achieved by employing the aforementioned connection between image processing and partial differential equations. Starting with pioneering works of Rudin (1987) and Perona & Malik (1987), nonlinear filtering based on nonlinear PDEs has become very useful in multiscale description of images, image segmentation, edge detection, image enhancement (Sapiro

2001). This approach is a state of art based on the design and analysis of PDEs. Perona and Malik (1987) proposed a nonlinear diffusion equation with the coefficient of diffusion D as a nonnegative function of the magnitude of local image gradient. The desirable D decays when the gradient grows and increases when the gradient decays. A different PDE was introduced by Rudin (1987) as means for nonlinear denoising of images without blurring sharp boundaries. He used a modification of a nonlinear equation describing evolution of shock waves (thus preserving or even sharpening objects). The approach suggested by Rudin had to deal with the following complications: the original equation was not symmetric in space, and it required a two-dimensional generalization. We use here an equation which was derived in Shrira and Pesenson (1983) (see also Pesenson 1991) to describe diffraction and stability of multi-dimensional shock waves and solitons. The equation has later become known as Shrira-Pesenson(SP) equation (Kivshar & Pelinovsky 2000). The SP equation can be written in the following form $I_{tt} - c^2\Delta I + (I_t^2 + I_y^2 + I_z^2)_t - \nabla(D\nabla I_t) = 0$. It turns out, that this equation naturally overcomes the aforementioned difficulties. Indeed, its two dimensional, rotationally invariant and thus, following Rudin (1987), can be used to develop a nonlinear filter.

3. Mosaics, Completeness and Reliability

Mosaics of two astronomical observation requests - AOR 3865856 and AOR 6070016 (NGC300) - are presented on Figures 1 and 2. Images were obtained by MIPS, 70 microns imaging band (Rieke et al. 2004). Mosaic size is 0.9 deg x 0.5 deg. Effective exposure time for one AOR is 30 sec. Effective exposure time for four AORs is 120 sec. Basic calibrated data (BCD) is from SSC pipeline version 10.0. Mosaic image is made by MOPEX (Makovoz & Khan 2004). There are three images in each figure, showing from top to bottom respectively - the mosaic before filtering, after a linear filtering (point sources are smeared), and the mosaic after the nonlinear filtering (point sources remain sharp). One of the goals of nonlinear filtering is to improve point source extraction. We applied point source extraction software included in MOPEX (Makovoz & Khan 2004), to a single AOR3865856 before and after filtering. The results were compared with a true list of sources from an image obtained by combining four AORs for the same field of view as AOR3865856. Figure 3 shows the completeness and Figure 4 shows the reliability of the point source extraction (the solid line corresponds to the filtered image, and the dashed line to the non-filtered image) vs. logarithm of true flux in μmJy. Here completeness is defined as the ratio of the number of matched sources to the number of true sources; reliability is defined as the ratio of the number of detected sources to the number of matched sources. The improvement is in the highest flux range, reaching 100% reliability.

4. Conclusion

It can be seen from the completeness and reliability plots (Figs. 3,4), that the nonlinear filtering ensures better completeness and reliability for higher fluxes. Stopping filtering at less coarse levels of scale (smaller times, in PDE's termi-

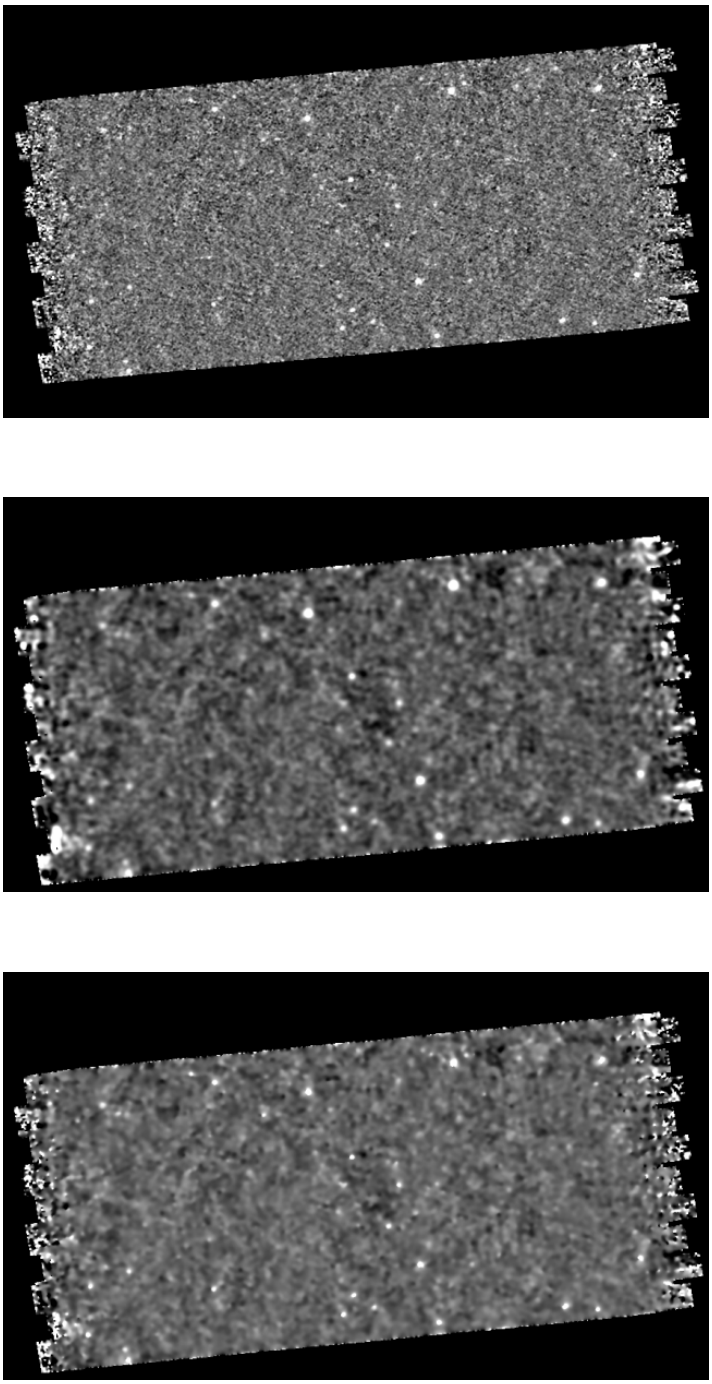

Figure 1. One AOR mosaic. From top to bottom - before filtering, after a linear filtering (point sources are smeared), and after the nonlinear filtering (point sources remain sharp).

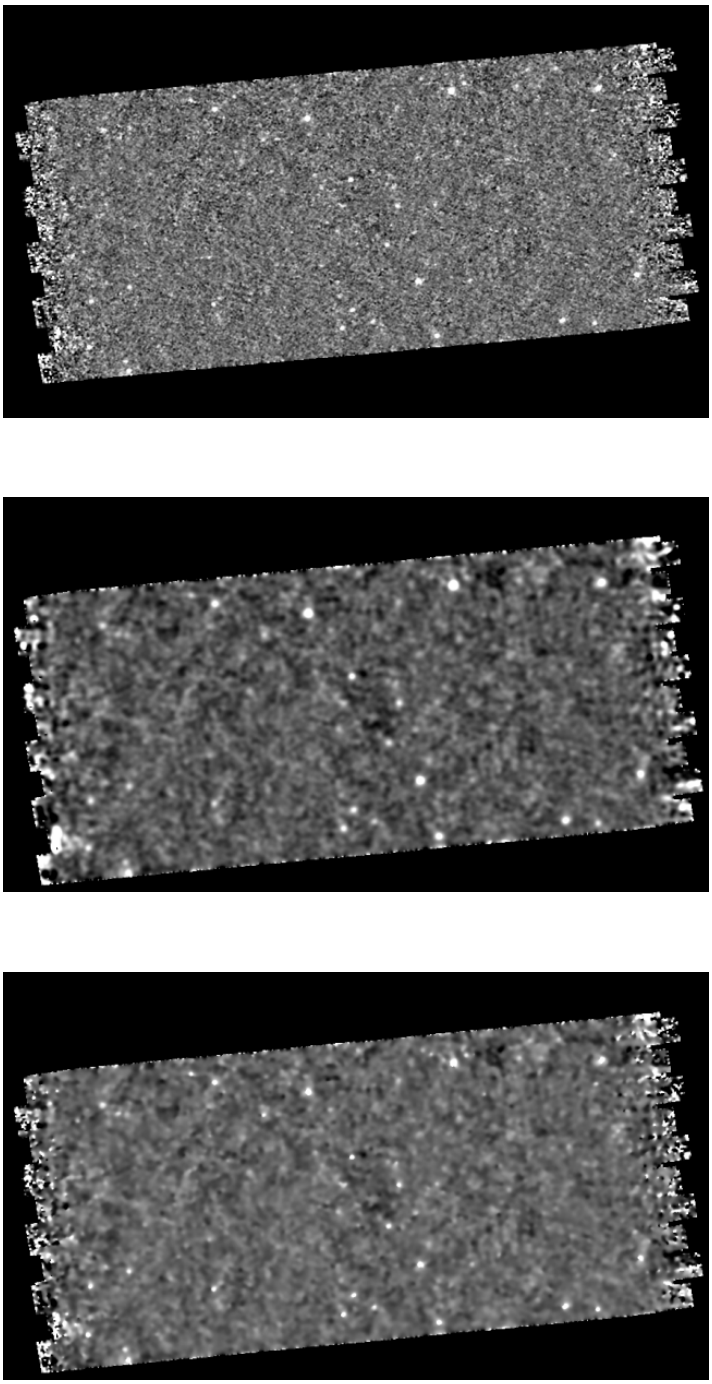

Figure 2. NGC300 mosaic. From top to bottom - before filtering, after a linear filtering (point sources are smeared), and after the nonlinear filtering (point sources remain sharp).

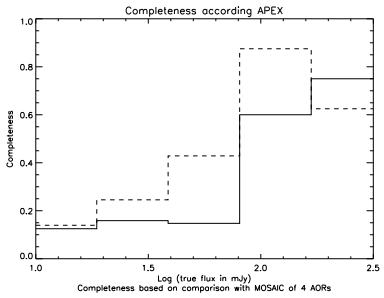

Figure 3. Completeness vs. log of true flux in μmJy.

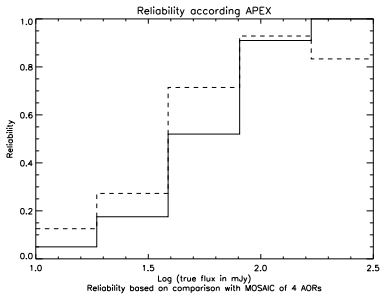

Figure 4. Reliability vs. log of true flux in μmJy.

nology) will increase completeness and reliability of the point source extraction at lower flux levels as well.

Acknowledgments. This work was carried out at the *Spitzer* Science Center, with funding from NASA under contract 1407 to the California Institute of Technology and the Jet Propulsion Laboratory. One of us (M.P.) wants to thank Tetsuyasu Uekuma for his insights and encouragement.

References

Kivshar, Y., & Pelinovsky, D. 2000, Physics Reports, 331, 117

Makovoz, D., & Khan, I. 2004, in ASP Conf. Ser., Vol. 347, ADASS XIV, ed. P. L. Shopbell, M. C. Britton, & R. Ebert (San Francisco: ASP), 81

Perona, P., & Malik, J. 1987, IEEE Trans. Pattern Anal. Mach. Intell., 12, 629

Pesenson, M. 1991, Physics of Fluids, A3, 12, 301

Rieke, G., et al. 2004, ApJS, 154, N1

Rudin, L. 1987, Images, Numerical Analysis and Shock Filters, Technical report 5250, CIT

Sapiro, G. 2001, Geometric Partial Differential Equations and Image Analysis (Cambridge University Press: England)

Shrira, V., & Pesenson, M. 1983, In Nonlinear and Turbulent Processes in Physics, Ed. R. Sagdeev, Vol. 2, (Harwood Academic, NY)

Witkin, A. 1983, In Proc. Intern. Conf. on Artificial Intelligence